Eur. Phys. J. D **31**, 107–112 (2004)
DOI: 10.1140/epjd/e2004-00123-2

THE EUROPEAN PHYSICAL JOURNAL D

Fluorescence from doubly driven four-level atoms

A density matrix approach

A. Narayanan[a], R. Srinivasan, U.K. Khan, A. Vudayagiri, and H. Ramachandran

Raman Research Institute, Sadashivnagar, Bangalore 560 080, India

Received 14 May 2004 / Received in final form 2 July 2004
Published online 21 September 2004 –

Abstract. The unusually narrow features in the fluorescence from ^{85}Rb driven by two laser fields L1 and L2, reported in [1], are explained on the basis of a four-level density matrix calculation. The L2 laser enables atom transfer to the fluorescing levels connected by the strong L1 laser. In turn the L1 laser causes the Autler-Townes splitting of the upper levels connected by L2 laser. These two effects are shown to maximise fluorescence within a narrow spectral range of the scanned L2 laser due to velocity selection of atoms from co-propagating and counter propagating L1 and L2 lasers. The analysis reveals the existence of narrow spectral features from a collection of atoms at room temperature even in the absence of induced coherences between the levels.

PACS. 42.50.Hz Strong-field excitation of optical transitions in quantum systems; multiphoton processes; dynamic Stark shift – 32.80.Bx Level crossing and optical pumping

1 Introduction

Multilevel atoms, under the action of multiple fields, display a variety of phenomena brought about by the ac Stark splitting of electronic levels and by interference due to induced coherences. These manifest themselves as splitting of peaks, inhibition of absorption or emission, narrow windows of transparency, etc. In particular, theoretical work on three level atoms have considered Λ, V and ladder type of three level systems [2]. The presence of additional levels increases multifold the possibilities of interference phenomena that exist. In this context, probing the ac Stark splitting of a doubly driven three level system by connecting it in absorption to a fourth level has been studied both theoretically and experimentally. The nested Λ, N systems, cascade systems have been examined [3–5]. Four level systems have also been studied in slightly varied contexts in examining interference between dark states [6] and in proposing a which path quantum eraser [7]. In all these studies interference between dressed states determines the width of the spectral feature studied. Even in an intrinsically *non–Doppler* free geometry [8], it is the interference effects which produce Doppler free line widths. In this paper we examine rigorously, using a density matrix formalism, an "inverted N" system containing four hyperfine levels of ^{85}Rb, driven by two lasers L1 and L2. The experimental result of narrow spectral features seen in fluorescence from this system [1] have prompted this study. Unlike earlier studies the transitions driven by these two lasers have no level in common. Our analysis shows that narrow spectral features are obtained even in the absence of interference effects. Velocity selection of atoms from co and counter propagating laser geometries, as in the case of cross-overs from multi-level atoms is seen to be the dominant mechanism of producing such novel narrow line widths from a dilute collection of room temperature atoms.

2 Experiment

The experiment in [1] consisted of driving a collection of ^{85}Rb atoms with two fields- a strong "L1" field and a weak "L2" field. The L1 and L2 laser were arranged in a 3-D optical molasses configuration, overlapping in all the six directions. Each L1 beam was of intensity 1 mW/cm^2, and the L2 0.1 mW/cm^2. The L1 laser was held at a fixed detuning δ_c from the conventional cooling transition $5S_{1/2}, F = 3 \rightarrow 5P_{3/2}, F' = 4'$ and the L2 laser was scanned with its detuning (δ_r) from $5S_{1/2}, F = 2 \rightarrow 5P_{3/2}, F' = 3'$ level varying over the entire manifold, $F = 2 \rightarrow F' = 1', 2', 3'$ (see Fig. 1)[1]. For most δ_c values, the temperature of the gas was 300 K. Narrow fluorescence peaks were observed at definite δ_r for a given δ_c. While one would expect a broad fluorescence, with the width indicative of the temperature of the gas, the experiment

[a] e-mail: andal@rri.res.in

[1] Hyperfine levels of $5S_{1/2}$ are denoted unprimed while that of $5P_{3/2}$ are denoted primed.

$$H = \begin{vmatrix} \hbar\omega_2 & 0 & -\frac{\hbar}{2}\Omega_{23'}e^{(-i\omega_{LR}t)} & 0 \\ 0 & \hbar\omega_3 & -\frac{\hbar}{2}\Omega_{33'}e^{(-i\omega_{LC}t)} & -\frac{\hbar}{2}\Omega_{34'}e^{(-i\omega_{LC}t)} \\ -\frac{\hbar}{2}\Omega_{23'}e^{(i\omega_{LR}t)} & -\frac{\hbar}{2}\Omega_{33'}e^{(i\omega_{LC}t)} & \hbar\omega_{3'} & 0 \\ 0 & -\frac{\hbar}{2}\Omega_{34'}e^{(i\omega_{LC}t)} & 0 & \hbar\omega_{4'} \end{vmatrix}$$

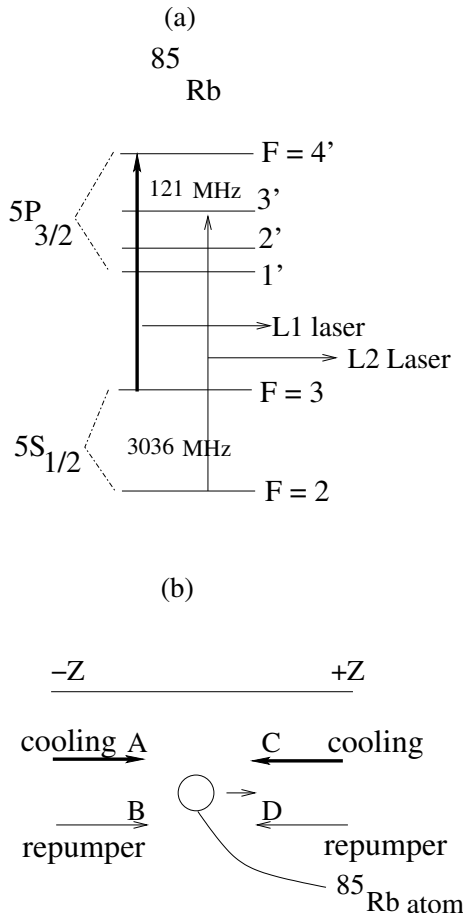

Fig. 1. (a) Energy level diagram of ^{85}Rb. (b) A one dimensional configuration (along **Z**) of the L1 and L2 beams with the ^{85}Rb atom taken move along $+z$-direction.

showed fluorescence peaks just 30 MHz in width, much smaller than their Doppler width of 500 MHz. This was explained using a numerical calculation, on the basis of a double resonance model which maximised fluorescence whenever the atom found both the L1 and L2 lasers on resonance with their respective transitions. A simple analytical treatment based on the above model showed that atom transfer efficiency by the L2 laser to the levels connected by the L1 laser was maximised under the double resonance condition and gave rise to narrow fluorescence peaks [1].

We give here a complete analysis of this system using a four-level density matrix formalism which reproduces all the features observed in the experiment.

3 Four level density matrix

The four levels under consideration are: the two ground hyperfine levels $F = 2, 3$ and the two excited levels $F' = 3', 4'$. For simplicity, we have considered an one dimensional situation where the two driving fields are in the $\pm z$-direction and the atom is moving along the z-direction with a velocity $\mathbf{v}$. The detuning of the L1 laser taking the Doppler effect into account is $\Delta_c = \delta_c - \mathbf{k}_c.\mathbf{v}$ and the L2 laser's detuning is $\Delta_r = \delta_r - \mathbf{k}_r.\mathbf{v}$ where, δ_c and δ_r are the detunings of the laser in the laboratory frame. The total Hamiltonian for the system consisting of the atom and the light fields is written in the interaction picture as

$$H = H_0 + H_I \tag{1}$$

where H_0 is the Hamiltonian for the bare atom and H_I is the atom-light interaction Hamiltonian. They are given as

$$H_0 = \hbar\omega_2|2\rangle\langle 2| + \hbar\omega_3|3\rangle\langle 3| + \hbar\omega_{3'}|3'\rangle\langle 3'| + \hbar\omega_{4'}|4'\rangle\langle 4'|$$

and

$$H_I = -\frac{\hbar}{2}[\Omega_{34'}|3\rangle\langle 4'|\exp(-i\omega_{LC}t) + \Omega_{33'}|3\rangle\langle 3'|\exp(-i\omega_{LC}t) + \Omega_{23'}\exp(-i\omega_{LR}t)|2\rangle\langle 3'| + H.C].$$

Here the $\hbar\omega_i$ represent the energies of the levels as represented in Figure 1, with $\hbar\omega_2$ taken as zero, ω_{LC} and ω_{LR} the frequencies of the L1 and L2 laser beams and $\Omega_{ij'}$ is the Rabi frequency connecting the levels i and j'. The total Hamiltonian can be written in matrix form as follows

see equation above

where the rows and columns correspond to levels $2, 3, 3', 4'$ in sequence. The dynamics of the system described by this Hamiltonian can be studied using the density matrix $\rho = \sum \rho_{ij}|i\rangle\langle j|$. The time evolution of the density matrix ρ is given by the Liouville equation

$$\frac{d\rho}{dt} = -\frac{i}{\hbar}[H, \rho] - \frac{1}{2}\{\Gamma, \rho\} \tag{2}$$

with

$$\Gamma_{ij'} = 2\gamma_{i\to j'}\delta_{ij'} \tag{3}$$

where $\gamma_{i\to j'}$ being the spontaneous decay rate from the j'th level to the ith level[2]. The rate equations of the four

[2] where $\Gamma_{ij'}$ is the decay rate of the level j' to the level i. This is however a diagonal matrix.

levels for an atom moving with a velocity v are derived under the rotating wave approximation. They are

$$\frac{d\rho_{22}}{dt} = -\frac{i}{2}[\Omega_{23'}\rho_{3'2} - \Omega^*_{23'}\rho_{23'}] + 2\gamma_{3'2}\rho_{33'} \quad (4)$$

$$\frac{d\rho_{23}}{dt} = -i(\Delta_{c3'} - \Delta_r)\rho_{23} - \frac{i}{2}[\Omega_{23'}\rho_{3'3} - \Omega^*_{33'}\rho_{23'} - \Omega^*_{34'}\rho_{24'}] \quad (5)$$

$$\frac{d\rho_{23'}}{dt} = (i(\Delta_r) - (\gamma_{3'2} + \gamma_{3'3}))\rho_{23'} - \frac{i}{2}[\Omega_{23'}\rho_{3'3'} - \Omega^*_{23'}\rho_{22} - \Omega^*_{33}\rho_{23}] \quad (6)$$

$$\frac{d\rho_{24'}}{dt} = -i[(\Delta_{c3'} - \Delta_c - \Delta_r) - i\gamma_{4'3}]\rho_{24'} - \frac{i}{2}[\Omega_{23'}\rho_{34'} - \Omega_{34'}\rho_{23}] \quad (7)$$

$$\frac{d\rho_{32}}{dt} = i(\Delta_{c3'} - \Delta_r)\rho_{32} - \frac{i}{2}[\Omega_{33'}\rho_{3'2} + \Omega_{34'}\rho_{4'2} - \Omega_{23'}\rho_{33'}] \quad (8)$$

$$\frac{d\rho_{33}}{dt} = -\frac{i}{2}[\Omega_{33'}\rho_{3'3} + \Omega_{34'}\rho_{4'3} - \Omega_{33'}\rho_{33'} - \Omega_{34'}\rho_{34'}] + 2\gamma_{3'3}\rho_{3'3'} + 2\gamma_{4'3}\rho_{4'4'}) \quad (9)$$

$$\frac{d\rho_{33'}}{dt} = (i\Delta_{c3'} - (\gamma_{3'2} + \gamma_{3'3}))\rho_{33'} - \frac{i}{2}[\Omega_{33'}\rho_{3'3'} + \Omega_{34'}\rho_{4'3'} - \Omega_{23'}\rho_{32} - \Omega_{33'}\rho_{33}] \quad (10)$$

$$\frac{d\rho_{34'}}{dt} = (i\Delta_c - \gamma_{4'3})\rho_{34'} - \frac{i}{2}[\Omega_{33'}\rho_{3'4'} + \Omega_{34'}\rho_{4'4'} - \Omega_{34'}\rho_{33}] \quad (11)$$

$$\frac{d\rho_{3'2}}{dt} = (-i\Delta_r - (\gamma_{3'2} + \gamma_{3'3}))\rho_{3'2} - \frac{i}{2}[\Omega^*_{23'}\rho_{22} + \Omega^*_{33'}\rho_{32} - \Omega^*_{23'}\rho_{3'3'}] \quad (12)$$

$$\frac{d\rho_{3'3}}{dt} = (-i\Delta_{c3'} - (\gamma_{3'2} + \gamma_{3'3}))\rho_{3'3} - \frac{i}{2}\Omega^*_{33'}\rho_{23} - \frac{i}{2}[\Omega^*_{33'}\rho_{33} - \Omega^*_{33}\rho_{3'3'} - \Omega_{34'}\rho_{3'4'}] \quad (13)$$

$$\frac{d\rho_{3'3'}}{dt} = -2(\gamma_{3'2} + \gamma_{3'3})\rho_{3'3'} - \frac{i}{2}\Omega^*_{33'}\rho_{3'3} - \frac{i}{2}[\Omega_{23'}\rho_{23'} + \Omega^*_{33'}\rho_{33'} - \Omega_{23'}\rho_{3'2}] \quad (14)$$

$$\frac{d\rho_{3'4'}}{dt} = [(i\Delta_{c3'} - \Delta_c) - (\gamma_{3'2} + \gamma_{3'3} + \gamma_{4'3})]\rho_{3'4'} - \frac{i}{2}[\Omega^*_{23'}\rho_{24'} + \Omega^*_{33'}\rho_{34'} - \Omega_{34'}\rho_{3'3}] \quad (15)$$

$$\frac{d\rho_{4'2}}{dt} = [(i\Delta_{c3'} - \Delta_c - \Delta_r) - \gamma_{4'3}]\rho_{4'2} - \frac{i}{2}[\Omega^*_{34}\rho_{32} - \Omega^*_{23'}\rho_{4'3'}] \quad (16)$$

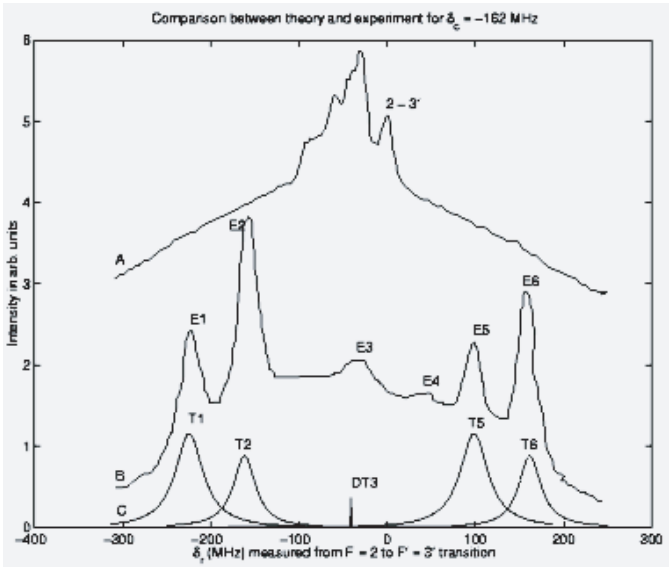

Fig. 2. Trace A shows the saturation absorption spectrum of L2. Trace B shows the experimental curve for a L1 detuning of $\delta_c = -162$ MHz. The E1-E6 labels represent the peak positions as found in the experiment. Trace C shows the result of the density matrix calculations for the same δ_c taking the levels $F = 2, 3$ and $F' = 3'(2')$ and $4'$ into account. The T1, T2, DT3, T5 and T6 labels the resultant theoretically derived peak positions.

$$\frac{d\rho_{4'3}}{dt} = [(i\Delta_c - \gamma_{4'3})]\rho_{4'3} - \frac{i}{2}[\Omega^*_{34}\rho_{33} - \Omega^*_{33'}\rho_{4'3'} - \Omega^*_{34'}\rho_{4'4'}] \quad (17)$$

$$\frac{d\rho_{4'3'}}{dt} = [-i(\Delta_{c3'} - \Delta_c) - (\gamma_{3'2} + \gamma_{3'3} + \gamma_{4'3})]\rho_{4'3'} - \frac{i}{2}[\Omega_{34'}\rho_{33'} - \Omega_{33'}\rho_{4'3} - \Omega^*_{23'}\rho_{4'2}] \quad (18)$$

$$\frac{d\rho_{4'4'}}{dt} = -\frac{i}{2}[\Omega^*_{34'}\rho_{34'} - \Omega_{34'}\rho_{4'3}] - 2\gamma_{4'3}\rho_{4'4'}. \quad (19)$$

Here $\delta_{c3'} = 2\pi 121$ MHz$+\delta_c$, 121 MHz being the hyperfine level separation of $3'$ level from $4'$. $\gamma_{3'2} = 2.0$ MHz and $\gamma_{4'3} = 6$ MHz, $\gamma_{3'3} = 2.6$ MHz. For each velocity **v** steady state values of ρ_{ij} are obtained by numerically solving the above rate equations for various values of δ_c and δ_r, subject to the constraint $\rho_{22} + \rho_{33} + \rho_{3'3'} + \rho_{4'4'} = 1$. Thus for an atom with a velocity **v** we obtain the population of each level and coherence between various levels for different values of δ_r and δ_c. The fluorescence emitted by atoms with a velocity **v** is given by

$$Fluorescence(\Delta_c, \Delta_r) = \Gamma_{4'3}\rho_{4'4'} + \Gamma_{3'3}\rho_{3'3'} + \Gamma_{3'2}\rho_{3'3'}. \quad (20)$$

As the detector collects fluorescence from atoms which are in thermal motion, we take the average of each ρ_{ij} value over the range of velocities, weighted by the one dimensional Maxwellian velocity distribution. The fluorescence calculated as above as a function of δ_r and the corresponding experimental data are given in Figure 2 for a L1 laser detuning $\delta_c = -162$ MHz. A general agreement between

the results of our calculation and that of the experiment is seen. The individual features will be discussed in detail below.

4 Discussion

Consider a situation shown in Figure 1b, when the L1 and L2 beams are both along $\pm z$-directions. Initially let us consider the atoms to be at rest. For a given detuning δ_c of the L1 (pump) laser, we should get fluorescence peaks corresponding to the Autler-Townes (AT) dressed states of $F' = 3'$ at L2 (probe) detunings [9]

$$\delta^0_{r\pm} = \frac{\delta_{c3'}}{2} \pm \sqrt{(\delta^2_{c3'} + \Omega^2)}/2. \tag{21}$$

Here $\delta_{c3'} = 2\pi * 121$ MHz $+ \delta_c$ denotes the detuning of the L1 laser from $3 \rightarrow 3'$ transition, 121 MHz being the level spacing between $F' = 3'$ and $4'$ levels and Ω its Rabi frequency. For the specific case shown in Figure 2, for a L1 laser detuning $\delta_c = -162$ MHz and for small Ω, the Autler-Townes peak positions for these zero velocity atoms are $\delta^0_{r\pm} \approx 0, -41$ MHz. This is confirmed from our density matrix calculations. At these detunings of the probe its absorption is maximised and repumping most efficient as seen from Figures 3a and 3b which give $\rho_{23'}$, ρ_{22} and ρ_{33} as functions of δ_r.

Consider now an atom in motion with a velocity $+v$, along the $+z$-direction. If $\delta_c < 0$ this atom predominantly absorbs from the L1 beam coming towards it (C in Fig. 1b). This causes AT splitting of the $F' = 3'$ level of this atom. As the L2 laser is scanned, the AT doublet levels of $F' = 3'$ will absorb the L2 beam from either B or from D depending on the sign of δ_r. Thus absorption of L2 will occur four times for a given δ_c of the L1 laser. The same holds for $\delta_c > 0$ for atoms with velocity $-v$.

The AT doublet positions at which absorption occurs in a frame where the atom is at rest are given by equations (21). However from the laboratory frame these positions will get Doppler shifted to

$$\delta_{r-} = \delta^0_{r-} - (kv) \approx -kv \tag{22}$$

$$\delta_{r+} = \delta^0_{r+} - (kv) \approx \delta_{c3'} \tag{23}$$

when L2 absorption happens from D

$$\delta_{r-} = \delta^0_{r-} + (kv) \approx +kv \tag{24}$$

$$\delta_{r+} = \delta^0_{r+} + (kv) \approx \delta_{c3'} + 2kv \tag{25}$$

when L2 absorption happens from B.

Thus, as the L2 laser is scanned, maximum transfer of population from $F = 2$ to $F = 3$ will occur when these conditions are satisfied for each velocity class of atoms. Now, as mentioned in [1] and as will be shown shortly, the fluorescence is predominantly from $4' \rightarrow 3$. However, not all atoms transfered to $F = 3$ will be in resonance with the L1 laser. Only a small velocity class around v_c satisfying $\delta_c - \mathbf{k}\cdot\mathbf{v}_c = 0$ will give rise to fluorescence. This velocity selection effect is confirmed by our calculations and is shown

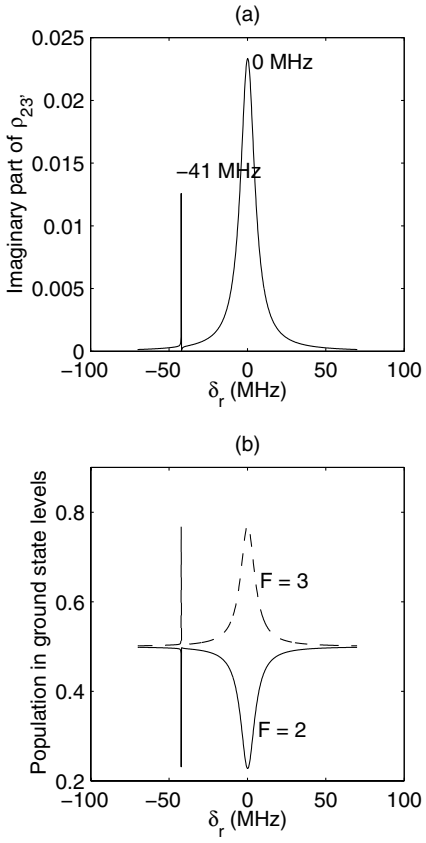

Fig. 3. The imaginary part of $\rho_{23'}$ vs. the positions of the probe absorption δ_r showing that absorption of the L2 laser light due to Autler-Townes splitting of the level $F' = 3'$ occurs at the detunings 0 MHz and -41 MHz. (b) ρ_{33} (dashed line) and ρ_{22} (full line) as functions of δ_r.

in Figure 4 which gives $\rho_{4'4'}$ and $\rho_{3'3'}$ as functions of the velocity of the atom for $\delta_c = \delta_r = -162$ MHz. We see that the population in $F' = 4'$ ($\rho_{4'4'}$) is two orders more than that in $F' = 3'$ ($\rho_{3'3'}$) and it peaks at the critical velocity $v_c = 126$ m/s. Therefore only for velocities around v_c will the fluorescence from $F' = 4'$ be maximised, showing that indeed the resonance condition ($\mathbf{k}\cdot\mathbf{v} = \delta_c$) selects a narrow velocity class for fluorescence.

So of the several multitude of Autler-Townes doublets of $F' = 3'$ given rise by L1 laser, corresponding to various velocities of the moving atoms, a particular pair corresponding to the velocity v_c satisfying the resonance condition, maximises fluorescence from $F' = 4'$. The peak positions of this AT pair (δ_r) are given by equations (22, 23, 24, 25), with the constraint that resonance should also be satisfied for maximum fluorescence. These are now given as

$$\delta_{r-} = \delta_c;\ \delta_{r+} = 121 \text{ MHz} + \delta_c \tag{26}$$

when L2 absorption takes place from D and

$$\delta_{r-} = -\delta_c; \quad \delta_{r+} = 121 \text{ MHz} - \delta_c (v = v_c); \tag{27}$$

$$\delta_{r+} = 121 \text{ MHz} + \delta_c + 2kv (v \neq v_c) \tag{28}$$

when L2 absorption takes place from B.

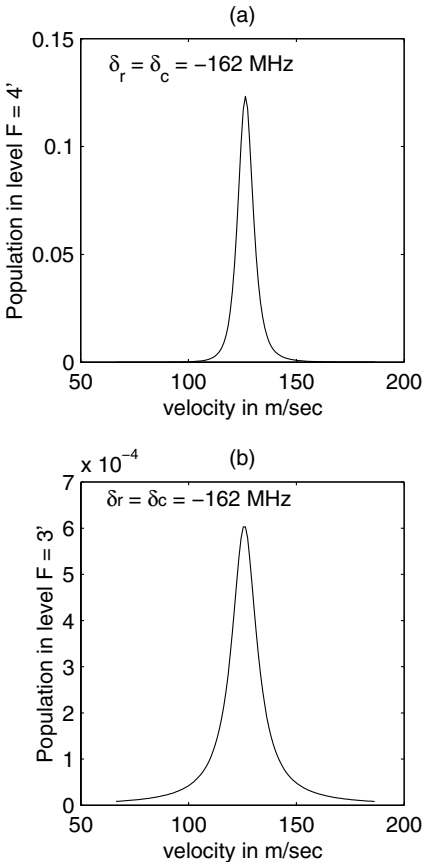

Fig. 4. Populations in the upper levels $F = 4'$ (a) and $F = 3'$ (b).

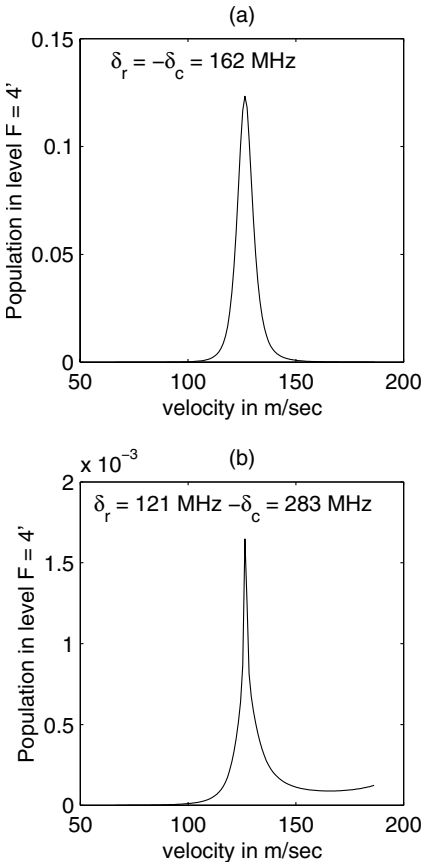

Fig. 5. Population in the level $F' = 4'$ as a function of the velocity of atoms for the Autler-Townes peaks at (a) $\delta_r = -\delta_c = 162$ MHz, (b) $\delta_r = 121$ MHz $- \delta_c = 283$ MHz.

These peak positions for $\delta_c = -162$ MHz will now be at -162 MHz (T2), -41 MHz (DT3), $+162$ MHz (T6) and 283 MHz (Fig. 2). We see that both experimentally and theoretically we get peaks at all the other positions, except at 283 MHz. The same peak positions are obtained for atoms with a velocity $-v$, for $\delta_c > 0$.

It has been estimated in [9] that the peak at δ_{r-} is broad and the one at δ_{r+} is narrow. The width of the AT peaks decide the prominence of a fluorescence peak as it decides the number of atoms transfered in the fluorescing levels. Thus for peak positions $\delta_{r-} = \delta_c$ & $-\delta_c$ we expect a large fluorescence whereas for the peak at $\delta_{r+} = 121$ MHz $+ \delta_c$ we expect a much smaller fluorescence as is indeed seen from experiment and from our calculations (Fig. 2).

The peak at 283 MHz around $\delta_{r+} = 121$ MHz$+\delta_c+2kv$ is absent both in experiment and in our density matrix calculation. For this case, the L2 absorption takes place from B whereas the L1 is absorbed from C. When the absorption takes place from counter-propagating L1 and L2 beams the velocity class satisfying the resonance condition is severely restricted. In fact only for $v = v_c$ will the resonance condition be satisfied. Atoms with $v \neq v_c$ will see the L1 and L2 to be shifted by different detunings and hence will not contribute to the fluorescence. Thus the peaks resulting from this configuration will not be resolvable as only a very small number of atoms contribute to it. The severely restricted velocity range at resonance resulting in the absence of the peak at 121 MHz$+\delta_c+2kv$ is illustrated in Figure 5b which is obtained from the density matrix calculation. As we see here, only a small number in a very narrow velocity range contribute to population in $F' = 4'$ in contrast to the case $\delta_{r-} = -\delta_c$ (Fig. 5a).

The peaks marked T1, DT3 and T5 in Figure 2 are the peaks corresponding to the AT levels of $F' = 2'$ corresponding to absorption from counter and co-propagating L2 beams. These peaks can be got from the same four-level density matrix calculation by replacing the level $F' = 3'$ by $F' = 2'$. Thus the peaks are obtained at

$$\delta_{r-} = \pm\delta_c = \pm 162 \text{ MHz} \tag{29}$$

$$\delta_{r+} = 184 \text{ MHz} + \delta_c = +22 \text{ MHz} \tag{30}$$

with 184 MHz being the hyperfine separation between $F' = 4'$ and $F' = 2'$ level. Here the detuning δ_r is measured from the $F' = 2'$ transition. But in the experimental scan we measured separations from $F' = 3'$. So in order to be consistent with the experiment we plot these peaks with their separations as measured from $F' = 3'$ transition. This gives rise to peaks T1 and T5 and another peak at the position of the DT3 peak of $F' = 3'$ transition (Fig. 2). It is seen that the peak positions of T1 and T5 can be simply obtained from the corresponding peaks

for $F' = 3'$ by shifting them by -63 MHz, this being the hyperfine separation between $F' = 3'$ and $F' = 2'$.

The theoretically calculated widths of the fluorescence peaks match the experimentally observed narrow width of about 30 MHz. It should be emphasised that this does not arise due to the cooling of atoms in the optical molasses like configuration but due to the existence of a velocity selection as discussed above. These fluorescence peaks are experimentally seen to be narrow even for blue detunings of the L1 beam where no cooling occurs and the atoms are at *room temperature*. The expected Doppler width at this temperature is several hundred MHz. The additional effects of cooling on these fluorescent peaks in a Doppler free beam geometry will be discussed elsewhere.

5 Conclusions

Existence of narrow fluorescence peaks in the absence of induced coherences in a doubly driven multi-level atomic system [1], has been explained using a four-level density matrix formalism. The theory finds that the fluorescence peak positions are given rise by the Autler-Townes (AT) splitting of levels $F' = 3'$ and $F' = 2'$, for atoms around a particular velocity class. The AT splitting is seen to occur due to the strong L1 laser and hence is dependent on its detuning δ_c. The optical pumping of atoms by L2 (which connects $F' = 3'$ and $F' = 2'$ from $F = 2$) into the fluorescing level connected by L1 ($F = 3$ to $F' = 4'$) and the maximisation of fluorescence, leads to velocity selection of atoms from a broad Maxwellian distribution at room temperature. The theory accounts for all the peaks seen in the experiment and also explains the experimental absence of the other two peaks. The widths and heights of the peaks agree quite well with the experimentally obtained widths and heights.

References

1. U.K. Khan et al., Europhys. Lett. **67**, 35 (2004)
2. S.E. Harris, Phys. Today **50**, 36 (1997) and references therein; A.S. Zibrov et al., Phys. Rev. Lett. **75**, 1499 (1995); E. Arimondo, *Progress in Optics*, edited by E. Wolf (Elsevier, Amsterdam, 1996), Vol. XXXV
3. S.N. Sandhya et al., Phys. Rev. A **55**, 2155 (1997)
4. Changjiang Wei et al., Phys. Rev. A **58**, 2310 (1998)
5. S.R. de Echaniz et al., Phys. Rev. A **64**, 013812 (2001)
6. M.D. Ludkin et al. Phys. Rev. A **60**, 3225 (1999)
7. Y. Abranyos et al., Phys. Rev. A **60**, R2618 (1999)
8. C.Y. Ye et al., Phys. Rev. A **65**, 043805 (2002)
9. G. Vemuri et al., Phys. Rev. A **53**, 2842 (1996)